Normal Paper ☐
Student Paper ☒
Young Engineer Paper ☐

Coplanar Maneuvers to Observe an Assigned Site Based on Satellite Viewing-Swath Geometry Analysis

Luyi Yang[1], Jin Zhang[1,*], Yazhong Luo[1] and Haiyang Li[1]

[1)] *College of Aerospace Science and Engineering, National University of Defense Technology, Deya Road 109, Changsha, Hunan, 410073, China*

Abstract

This paper presents an iteration solution for the satellite's impulsive maneuvers to visit a target terrestrial site based on viewing-swath geometry analysis. Firstly, from spherical trigonometric formula, the viewing-swath is defined and the condition that the swath could cover a specified site is presented. Secondly, the effect of a coplanar impulsive maneuver under J2-perturbed dynamics on the swath's movement is analyzed. Thirdly, one-impulse and two-impulse solutions are proposed using an iteration method to improve the solution to high precision. Numerical results found that the proposed iteration method using swath geometry analysis could make the satellite satisfy the observation condition effectively and cost low fuel.

Key Words: Earth Observation, Viewing-Swath, Orbital Maneuver, Iteration Solution

1. Introduction

The LEO satellite plays an important role in Earth observation and orbital maneuvers are often required to adjust the ground track to cover one user-specified site, which is much more inexpensive than launching a new satellite [1].

According to thrust magnitude of propulsive maneuvers, the present researches can be divided into two categories: low thrust propulsion and impulsive propulsion. For the low thrust propulsion, [2] indicated that it was practical using electronic propulsion (EP) for a low circular orbit satellite to pass by the selected site within 50 days. Newberry [3] found that EP engine could make a typical satellite produce 24 hours earlier or later within 7 days to visit the site. Co et al. [4] [5] quantified reachability of a LEO satellite with impulsive or electronic propulsion and numerical terrestrial distance equations were derived based on time variable. For the method using impulsive maneuvers, totally it can be classified into two categories: the numerical approach and the approximately-analytical approach. Zhu et al. [6] used particle swarm optimization and differential evolution algorithm to optimize the transfer trajectory. Zhang [7] derived approximate analytical solutions including one-impulse and two-impulse maneuvers. Cases of both overflight and conical sensor were considered. An approximate solution was also provided to adjust the ground track to an assigned final orbit in [8]. Lin [9] studied the entire flight trajectory design of a spacecraft to operate a responsive mission. In [10] [11] genetic algorithms were used for orbit design in ground surveillance and temporary reconnaissance missions.

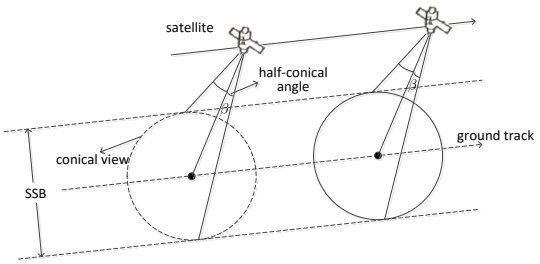

Fig. 1: Formation of viewing-swath by conical sensor

Present studies payed much attention to optimization algorithms or approximate analytical solutions but the method by geometric analysis is rarely studied. The satellite is equipped with an

*Corresponding author at: National University of Defense Technology, Changsha 410073, China
Email address: zhangjin@nudt.edu.cn

optical sensor in conical scan, which could form a viewing-swath on the Earth, seen in Fig 1. The purpose of this paper is to present a quick iterative solution for satellite's required impulses using swath geometry analysis.

2. Swath Geometric Relationship

2.1. Positions of Swath Vertices

Seen in Fig.2, a satellite flies over a sub-satellite point (SSP) *S* with a half-conical angle β, where the right view line intersects the Earth surface at Point $Q(\lambda_Q, \varphi_Q)$ .References[12] gives latitude φ_Q and longitude λ_Q by

$$\sin\varphi_Q = \cos\overline{SQ}\bullet\sin i\sin u - \sin\overline{SQ}\bullet\cos i \quad (1)$$

$$\tan\lambda_Q = \cos i\sin u + \sin i\tan\overline{SQ}/\cos u \quad (2)$$

$$\overline{SQ} = \sin^{-1}(r/r_e\bullet\sin\beta) - \beta \quad (3)$$

where *i* is the orbital inclination, *u* is the argument of latitude, *r* is the geocentric distance, and $\overline{SQ}$ is the projection arc length of the sensor view on the Earth surface.

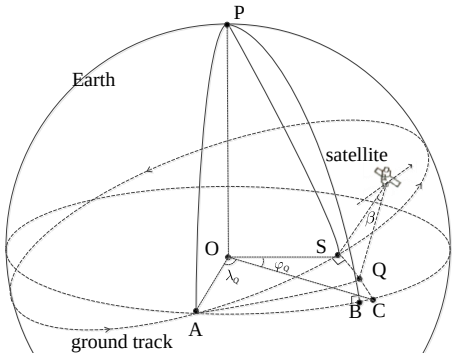

Fig. 2: Geometric relationship between SSP and intersecting point Q

Corresponding to $\overline{SQ}$=0 , the geocentric latitude φ_S and longitude λ_S of *S* satisfy

$$\sin\varphi_S = \sin i\sin u \quad (4)$$

$$\tan\lambda_S = \cos i\tan u \quad (5)$$

2.2. Swath Width along with Latitude

The swath width is defined as the longitude difference between latitude line endpoints, e.g. Q_E and Q_W in Fig. 3. And the swath is divided into three segments: *AB*, *BC* and *CD*:

(1) In *AB* segment, the west edge is selected at Point *A* and the east edge is selected at Q_E.

(2) In *BC* segment, the west and east edges are selected at the points Q_E and Q_W respectively.

(3) In *CD* segment, the west edge is selected at Q_W and the east edge is selected at Point *D*.

Q_E and Q_W are rolling points of S_1 and S_2. By setting $\varphi_{Q_E} = \varphi_S$, the argument of latitude u_E for S_1 and u_W for S_2 are expressed by

$$u_E = \sin^{-1}\left(\frac{\sin u}{\cos\overline{SQ}} + \frac{\tan\overline{SQ}}{\tan i}\right) \quad (6)$$

$$u_W = \sin^{-1}\left(\frac{\sin u}{\cos\overline{SQ}} - \frac{\tan\overline{SQ}}{\tan i}\right) \quad (7)$$

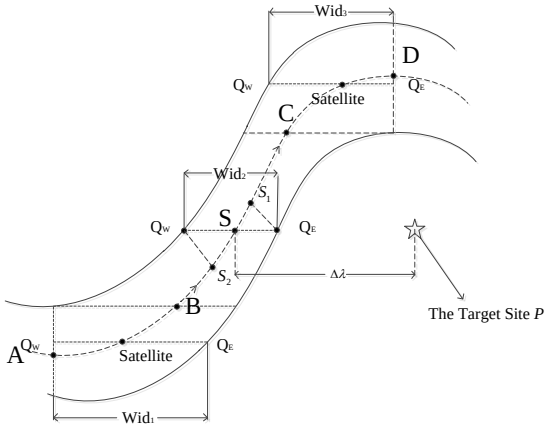

Fig. 3: Geometry of Swath's vertices and width

Then swath width could be obtained by

$$Wid = \begin{cases} \tan^{-1}\left(\dfrac{\cos i\sin u_E + \sin i\tan\overline{SQ}}{\cos u_E}\right) - \dfrac{3}{2}\pi, in\overline{AB} \\ \tan^{-1}\left(\dfrac{\cos i\sin u_E + \sin i\tan\overline{SQ}}{\cos u_E}\right) - \\ \tan^{-1}\left(\dfrac{\cos i\sin u_W - \sin i\tan\overline{SQ}}{\cos u_W}\right), in\overline{BC} \\ \dfrac{1}{2}\pi - \tan^{-1}\left(\dfrac{\cos i\sin u_W - \sin i\tan\overline{SQ}}{\cos u_W}\right),, in\overline{CD} \end{cases} \quad (8)$$

2.3. Observation Condition to Cover a Site

When satellite $S(\varphi_S, \lambda_S)$ arrives at the same latitude as the assigned site $P(\varphi_0, \lambda_0)$, there is

$$\varphi_S = \varphi_0 \quad (9)$$

Combining Eq. (1) and Eq. (4), the argument of latitude u_0 could be expressed by

$$u_0 = \sin^{-1}(\sin\varphi_0/\sin i) \quad (10)$$

It can be found that u_0 is determined by *i* and φ_0, which is considered to be time-invariant. In Fig. 3, the target could be observed on condition that

$$Wid/2 \geq \Delta\lambda \quad (11)$$

where *Wid* is swath width and $\Delta\lambda = \lambda_S - \lambda_0$ is longitude difference between Point *S* and *P*.

3. Coplanar Orbital Maneuver to Observe a Target Site

The following nomenclature is adopted: The subscript 1 indicates the initial orbit and the subscript 2 indicates the maneuvered orbit.

3.1. Influence of Maneuver on Swath

The orbital maneuver's influence includes two parts: swath movement and swath width.

Firstly, for the swath movement, under J_2 perturbation with a given impulse v_t, Ref. [13] gives the approximate expression of the SSP longitude difference in drifting time

$$\begin{aligned}\Delta\lambda &\approx [\Delta\dot{\Omega}_{J_2} + (\omega_e - \dot{\Omega}_{J_2})\frac{\Delta n_{J_2}}{n_{J_2}}(1-\frac{\Delta n_{J_2}}{n_{J_2}})]t \\ &= [\Delta\dot{\Omega}_{J_2} + (\omega_e - \dot{\Omega}_{J_2})\frac{\Delta n_{J_2}}{n_{J_2}}(1-\frac{\Delta n_{J_2}}{n_{J_2}})]\frac{u}{n_{J_2}}\end{aligned} \quad (12)$$

where n_{J_2} is the mean orbital velocity, Δn_{J_2} is the difference in n_{J_2}, $\dot{\Omega}_{J_2}$ is the drifting rate of RAAN, $\Delta\dot{\Omega}_{J_2}$ is the difference in $\dot{\Omega}_{J_2}$, *u* is the argument of latitude given by Eq. (9). Equation (12) indicates that an acceleration impulse results in swath eastwards movement, while a deceleration impulse results in westwards movement.

Secondly, for swath width, the variation is expressed by

$$\Delta Wid = Wid_2(u, i, \overline{SQ_2}) - Wid_1(u, i, \overline{SQ_1}) \quad (13)$$

And Eq. (13) is rewritten by

$$\Delta Wid \approx (\partial Wid / \partial v) \bullet \Delta v \quad (14)$$

where the differential expression $\partial Wid / \partial v$ could be obtained by numerical methods.

3.2. Coplanar One-Impulse Maneuver

The closest distance between the site $P(\varphi_0, \lambda_0)$ and SSP $S(\varphi_S, \lambda_S)$ should be obtained. Under J_2 perturbation λ_S is given by

$$\lambda_S = \Omega_0 + \lambda_S^{'} - \alpha_G + \dot{\Omega}_{J_2} \bullet t - \omega_e \bullet t \quad (15)$$

where $\lambda_S^{'} = \tan^{-1}(\cos i \tan u_0)$, ω_e is the mean rotation rate of the Earth, α_G is the Greenwich Mean Sidereal Time at time *t*. The flight time *t* is

$$t = (u_0 + 2k\pi)/n_{J_2} \quad (16)$$

where $k = 0, 1, 2, 3...$ is the revolution number after the satellite passes *P* for the first time. Substituting Eq. (16) into Eq. (15) and setting $\lambda_S = \lambda_0$, *k* is obtained as

$$k = \frac{1}{2\pi}[\frac{(\lambda_0 - \Omega_0 - \lambda_S^{'} + \alpha_G)n_{J_2}}{\dot{\Omega}_{J_2} - \omega_e} - u_0] \quad (17)$$

Due to the rotation of the Earth, λ_0 could be rewritten as

$$\lambda_0 = \lambda_0 + (N-1) \times 2\pi, N = 1, 2, 3... \quad (18)$$

Substituting Eq. (18) into Eq. (17) yields

$$k = \frac{1}{2\pi}[\frac{(\lambda_0 + (N-1) \times 2\pi - \Omega_0 - \lambda_S^{'} + \alpha_G)n_{J_2}}{\dot{\Omega}_{J_2} - \omega_e} - u_0] \quad (19)$$

Let k_N^* be the largest integer number that is no larger than the right-hand side in Eq. (19). The minimum longitude difference is expressed by

$$\begin{aligned}\Delta\lambda_N^* &= \Omega_0 + \tan^{-1}(\cos i \tan u_0) - \alpha_G \\ &+ (\dot{\Omega}_{J_2} - \omega_e)\frac{u_0 + 2k_N^*\pi}{n_{J_2}} - [\lambda_0 + (N-1) \times 2\pi]\end{aligned} \quad (20)$$

When $\Delta\lambda_N^* > 0$, an acceleration impulse is required to move swath westwards, which is called backward-phasing process.

When $\Delta\lambda_N^* < 0$, a deceleration impulse is required to move swath eastwards, which is called forward-phasing process.

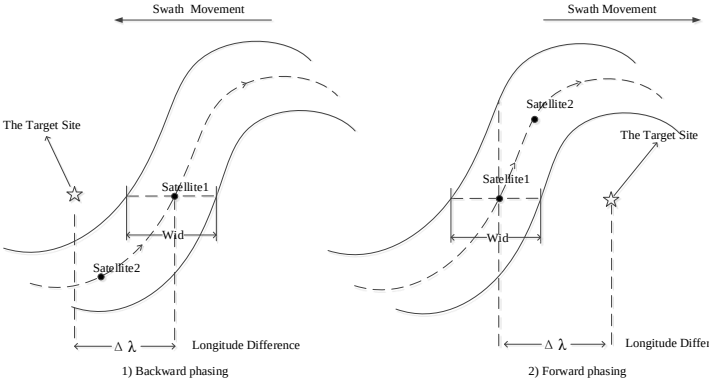

Fig. 4: Sketch of phasing process

Combining (20) with (11) (12), the after-maneuvered observation condition is rewritten as

$$\Delta\lambda_N^* - \Delta\lambda \leq (Wid_N + \Delta(Wid_N))/2 \quad (21)$$

or

$$-\Delta\lambda_N^* + \Delta\lambda \le (Wid_N + \Delta(Wid_N))/2 \quad (22)$$

3.3. Coplanar Two-Impulse Maneuver

The two-impulse problem is transformed to generate a required difference $\Delta\theta_k$ in the argument of latitude. Two coplanar in-track impulses are arranged as follows:

(1) The first impulse v_{t1} occurs at t=0, k revolutions away from the terminal point;

(2) The second impulse v_{t2} occurs at k-0.5 revolutions away from the terminal point.

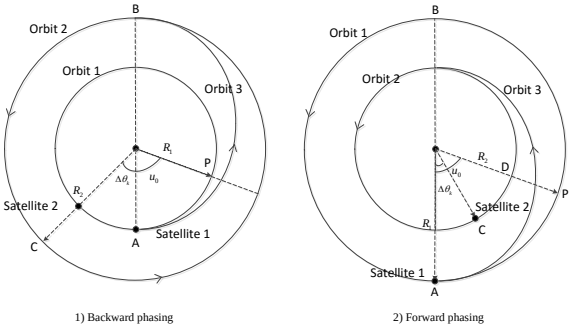

Fig. 5: Sketch of two-impulse phasing process

The target site will be observed in the (k+1)th revolution. Then Eq. (11) can be rewritten as:

$$\frac{Wid_N + \Delta(Wid_N)}{2} \ge \Delta\lambda_N^* - \frac{\omega_e}{n_1}\left(\frac{u_0 + \Delta\theta_k}{n_2} \times n_1 - u_0\right) \quad (23)$$

or

$$\frac{Wid_N + \Delta(Wid_N)}{2} \ge -\Delta\lambda_N - \frac{\omega_e}{n_1}\left(-\frac{u_0 - \Delta\theta_k}{n_2} \times n_1 + u_0\right) \quad (24)$$

where n_1 and n_2 are the mean orbital angular rate. The whole phasing process is similar to the Homan Transfer. For a specific $\Delta\theta_k$ under J_2 perturbation, [15] gives the two impulses by

$$v_{t1} = \Delta\theta_k / \left(\frac{6k\pi}{v_1} - \frac{21k\pi J_2 r_e^2 \cos i}{a^3 \omega_e}\right) \quad (25)$$

$$v_{t2} = n_1 a_1 e_1 / (2\sqrt{1-e_1^2}) \quad (26)$$

where a_1, v_1, and e_1 are the mean orbital elements before maneuvering.

3.4. Iteration Method

Combining Eqs. (21) to (24) with the numerical integration process, the required velocity increment *v* can be quickly calculated out.

Take Eq. (21) as an example and the objective variable value should be $q = \Delta\lambda + \Delta Wid_N/2$. It is a function of velocity impulse

$$q = H(v) \quad (27)$$

First-order variation of Eq. (27) is

$$\delta q = \nabla H \bullet \delta v \quad (28)$$

where $\nabla H = \partial q/\partial v = \partial(\Delta\lambda)/\partial v + \partial(\Delta Wid_N)/\partial v$ is obtained through numerical iteration. The expected objective is $q_{expected} = \Delta\lambda_N^* - Wid_N/2$. If *v* is given, the difference between the expected and corresponding objective value can be obtained by $\delta q = q_{expected} - q$ and v is corrected by

$$\delta v = \nabla H^{-1} \bullet \delta q \quad (29)$$

The iteration process is similar to the differential-correction method and usually a converged *v* could be obtained within five steps.

4. Numerical examples

To validate the proposed strategy, the same numerical example as Ref. [7] is used. The initial time is July 1, 2015 at 08:00:00 and flight time is 7 days. The city Wenchuan $(103.4^\circ E, 31^\circ N)$ is selected as the target site. The half-conical angle and swath width is $\beta = 30^\circ, Wid = 4.9445^\circ$. The initial orbital elements are $a = 6771.393km$, $e = 0, \Omega = 0^\circ, i = 97.0346^\circ, u = 0^\circ$.

4.1. One-impulse maneuver solution

Table 1 gives the results of one-impulse maneuver. On the first day, impulses for the ascending and descending stages are -100.75m/s and 60.76m/s. Compared with 253.08m/s and 63.32m/s in Ref. [7], it is reduced by 152.34m/s (60.19%) and 2.46m/s (3.88%) respectively. Especially in the ascending stage, the significant difference is due to the different phasing strategy. The forward-phasing strategy is chosen here while Ref. [7] used the backward-phasing strategy. The two minimum longitude differences are -7.575° and 15.735° on the first day. Therefore, the former one should be selected with a deceleration impulse maneuver. Fig. 6 shows that Ref. [7] has less fuel cost on the 3rd day and in the ascending stage on the 6th day but consumes more fuel from 152.34m/s to 1.84m/s in the other seven stages.

It can be also found that the total velocity increment decreases over time since the longitude difference in SSP varies almost linearly with time

t as given in Eq. (12). Width difference is within 1° in most stages, which is less than longitude difference $\Delta\lambda$. Therefore, swath movement contributes more than swath width in the maneuver process.

Table 1: One-impulse velocity increment

Day	Stage	v_t	$\Delta\lambda_N(^\circ)$	$\Delta\lambda_N+\Delta\lambda(^\circ)$	$Wid^{'}(^\circ)$
1	A	-100.75	-7.459	-2.286	4.579
	D	60.79	11.276	3.728	7.533
2	A	12.62	4.927	2.466	4.984
	D	0.00	0.507	/	/
3	A	-10.11	-5.841	-2.423	4.893
	D	-19.88	-10.110	-1.998	4.101
4	A	8.68	6.545	2.462	4.997
	D	0.00	2.275	/	/
5	A	0.00	-2.223	/	/
	D	-8.92	-8.493	-2.222	4.557
6	A	7.62	8.313	2.486	5.007
	D	1.78	3.892	2.462	5.023
7	A	0.00	-2.455	/	/
	D	0.00	-1.725	/	/

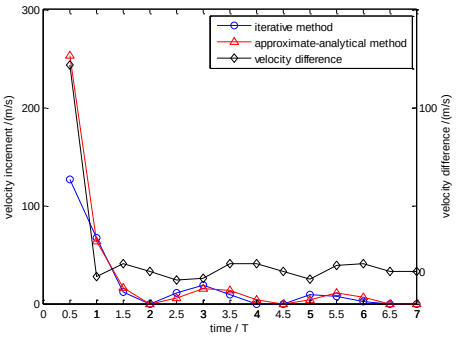

Fig. 6: Comparison of one-impulse strategy

For the LEO satellite, swath width increases with latitude from 5° to 28°, as shown in Fig. 7. Width difference almost increases linearly with the velocity impulses. The higher the impulse is, the larger the gradient is, as shown in Fig. 8.

Table 2: Velocity increment for different sites

Stage	$v_t(m/s)$	$\Delta\lambda_N(^\circ)$	$Wid^{'}(^\circ)$	$\Delta\lambda_N(^\circ)$	$Wid^{'}(^\circ)$
Wen	-100.75	-7.534	4.929	-100.75	-2.286
Site 1	-93.5	-7.514	6.001	-93.50	-2.593
Site 2	-75.47	-7.575	8.657	-75.47	-3.469
Site 3	/	-7.520	18.39	/	/
Wen	12.62	4.852	4.939	12.62	2.466
Site 1	9.88	4.857	6.021	9.88	2.994
Site 2	3.54	4.930	8.620	3.54	4.306
Site 3	/	5.164	18.20	/	/

Therefore, another three sites named *Site 1, Site 2* and *Site 3* are set to discuss site latitudes' influence on the maneuver impulse. The geographical positions are $(45^\circ N, 99.6^\circ E)$, $(60^\circ N, 93.3^\circ E)$, $(75^\circ N, 77.2^\circ E)$ respectively, which enable them to have the similar longitude difference with SSP before maneuvering. The flight duration limit is 2 days.

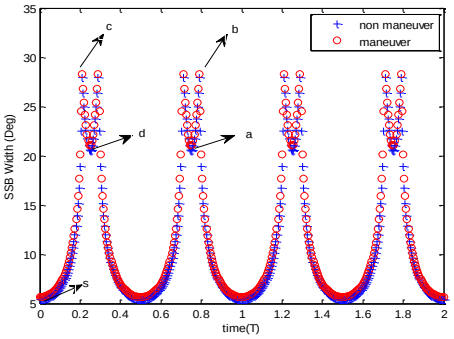

Fig. 7: Swath widths with and without maneuver

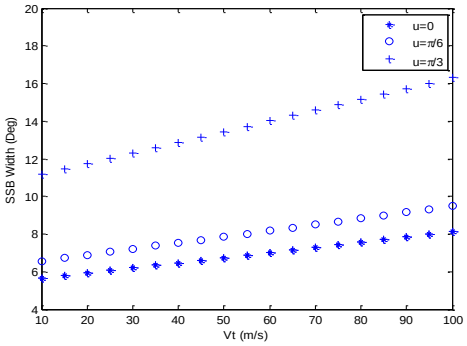

Fig. 8: Swath width's variation with impulses

It can be found that the required impulses decrease significantly with the site's latitudes, which is caused by difference in swath width. At Wenchuan the width is 4.92942° while at *Site 3* the width is 18.3878°. According to Eq. (22), this makes it easier to observe the target site. Especially for *Site 3* the width is wide enough so no maneuver is required. Therefore, less fuel is consumed to observe the site at higher latitude compared with the one at lower latitude.

4.2. Two-impulse maneuver solution

Table 3 gives the results of two-impulse maneuver adjustment. On the first day, velocity increment for the ascending and descending stages are -126.86m/s and 66.93m/s respectively, which are much lower than 222.47m/s and 78.06m/s in Ref. [7]. Especially for the ascending stage, the velocity cost is reduced approximately 42.98% because the phasing strategy is different again. Comparison of velocity increments in the next few days is shown in Fig. 9.

It can be found that on the 3rd day and in the ascending stage on the 6th day, Ref. [7] has less fuel cost. However, in the other seven stages the proposed iteration method consumes less velocity increment, from 95.61m/s to 4.81m/s. The fuel

cost is reduced by 30% on average.

Table 3: Two-impulse velocity increment

Day	Stage	v_{t1} m/s	v_{t2} m/s	v_{tol} m/s
1	A	-63.30	-63.56	-126.86
1	D	33.45	33.38	66.83
2	A	6.13	6.12	12.25
2	D	0.00	0.00	0.00
3	A	-5.48	-5.48	-10.96
3	D	-9.63	-9.64	-19.27
4	A	4.46	4.46	8.92
4	D	0.00	0.00	0.00
5	A	0.00	0.00	0.00
5	D	-4.48	-4.48	-8.96
6	A	3.83	3.83	7.66
6	D	0.95	0.95	1.90
7	A	0.00	0.00	0.00
7	D	0.00	0.00	0.00

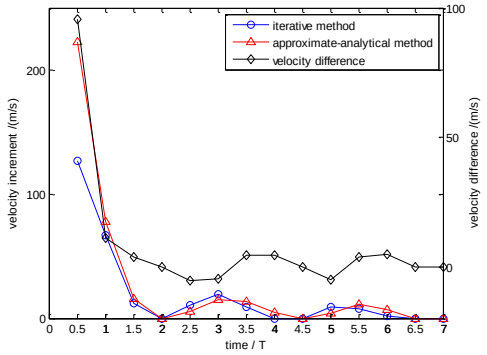

Fig. 9: Comparison of two-impulse strategy

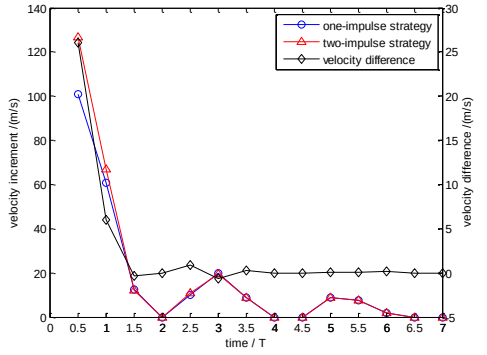

Fig. 10: Comparison of one-impulse and two-impulse strategy

Also, Figure. 10 compares one-impulse with two-impulse strategy. It is noticed that for one-impulse strategy velocity increment is usually smaller than that of two-impulse strategy, especially on the first day. The main reason is that the latter one needs to take two in-track impulses to keep the orbit shape circular while the former one does not.

5. Conclusion

This paper provides an iteration solution to the satellite's required impulses to visit a given terrestrial site and proposes swath geometry analysis method. Compared with approximate-analytical methods in [7], the proposed geometric analysis method shows better performance in fuel consumption. Instead of complicated algorithms and extensive computation, the proposed iteration method could quickly calculate out the required impulses. It is also found that acceleration strategy usually consumes less fuel than deceleration one. And it is easier to move viewing-swath to cover sites in high latitudes than ones in low latitudes. These findings help thoroughly understand the geometric relationship between the ground track and the terrestrial site.

Acknowledgements

This work was partly supported by the Science and Technology on Space Intelligent Control Laboratory (No. ZDSYS-2017-02), the National Science Foundation of China (No. 11572345 and No. 11472301).

References

1) Mcgrath, C. N. and Macdonald, M: Analytical Low-Thrust Satellite Maneuvers for Rapid Ground Target Revisit, *AIAA Space*, 2016.
2) Guelman, M. and Kogan, A.: Electric Propulsion for Remote Sensing from Low Orbits, *J Guid Control Dyn.*, **22**(1971), pp.313-321.
3) Newberry, R.: Powered Spaceflight for Responsive Space Systems, *High Frontier*, **4**(2004), pp. 48.
4) Co, T. C., Zagaris, C. and Black, J. T.: Responsive Satellites Through Ground Track Manipulation Using Existing Technology, *AIAA Space*, 2011.
5) Co, T. C. and Black, J. T.: Responsiveness in Low Orbits Using Electric Propulsion, *J of Spacecraft Rockets*, **51**(2014), pp. 938-945.
6) Zhu, K. J. and Baoyin, H. X.: Satellite scheduling considering maximum observation coverage time and minimum orbital transfer fuel cost, *Acta Astronaut.*, **66** (2010), pp. 220-229.
7) Zhang, G., Cao, X. B. and Mortari, D.: Analytical approximate solutions to ground track adjustment for responsive space, *IEEE Trans on Aerosp Electron System.*, **52** (2016), pp. 1366-1383.
8) Zhang G. and Sheng, J.: Impulsive Ground-Track Adjustment for Assigned Final Orbit., *J of Spacecraft Rockets*, **53** (2016), pp. 1-11.
9) Lin, M. P. and Xu, M.: Entire Flight Trajectory Design for Temporary Reconnaissance Mission, *Trans of the Japan Society Aeronaut Space Sci.*, **60**(2017), pp. 137-151. .
10) Kim, H. D., Bang, H. and Jung, O. C: Genetic Design of Target Orbits for a Temporary Reconnaissance Mission, *J of Spacecraft Rockets.*, **45**(2015), pp. 725-728.
11) Abdelkhalik, O., and Mortari, D.: Orbit Design for Ground Surveillance Using Genetic Algorithms, *J Guid Control Dyn.*, **29**(2015), pp. 1231-1235.
12) Zhang, H. B.: Theories and Methods of Spacecraft Orbital Mechanics, *National Defense Industry Press.*, 2013, pp. 238.
13) Zhang, J. Li, H. Y. amd Luo, Y. Z.: Effects of In-Track Maneuver on the Ground Track of Near-Circular Orbits, *J Guid Control Dyn.*, **37**(2015), pp. 1373-1378.
14) Zhang, J., Wang, X., Ma, X. B., Tang, Y. and Huang, H. B.: T Spacecraft long-duration phasing maneuver optimization using hybrid approach, *Acta Astronaut.*, **72** (2012), pp. 132-142.